

**A simple procedure for optimal scale-up of fine chemical processes.**

**Part II: the nitration of 4-chloro benzotrifluoride.**

Journal:	<i>Industrial &amp; Engineering Chemistry Research</i>
Manuscript ID:	ie-2008-00466n.R2
Manuscript Type:	Article
Date Submitted by the Author:	21-Nov-2008
Complete List of Authors:	Rota, Renato; Dip. di Chimica Materiali e Ingegneria Chimica, Politecnico di Milano Copelli, Sabrina; Politecnico di Milano, Maestri, Francesco; Politecnico di Milano, Gigante, Lucia; Stazione Sperimentale per i Combustibili, Lunghi, Angelo; Stazione Sperimentale per i Combustibili, Cardillo, Paolo; Stazione Sperimentale per i Combustibili,

SCHOLARONE™  
Manuscripts

# A simple procedure for optimal scale-up of fine chemical processes.

## Part II: the nitration of 4-chloro benzotrifluoride.

**Francesco Maestri, Sabrina Copelli, Renato Rota\***

Politecnico di Milano  
Dip. di Chimica, Materiali e Ingegneria Chimica "G. Natta"  
via Mancinelli 7 - 20131 Milano - Italy  
fax: +39 0223993180; e-mail: [renato.rota@polimi.it](mailto:renato.rota@polimi.it)

**Lucia Gigante, Angelo Lunghi, Paolo Cardillo**

Stazione Sperimentale per i Combustibili  
viale De Gasperi 3 - 20097 San Donato Milanese - Milano - Italy

### Abstract

In this work a simple and general procedure, for optimally scaling-up exothermic semibatch processes, has been applied to the analysis of a nitration reaction performed in the agrochemical industry for the production of an important class of herbicides. Such a reaction is performed in indirectly cooled semibatch reactors in which the species to be nitrated is added to a mixture of sulfuric and nitric acid, forming an heterogeneous (liquid-liquid) system. Adiabatic calorimetric experiments performed in an ARC equipment showed that the reaction in question belongs to the most critical class of exothermic reaction processes, for which maximum attainable temperature due to synthesis reaction (MTSR) is, at the same time, higher than system decomposition temperature and lower than boiling temperature of the reaction mass. It has been verified, through reaction calorimetry experiments (performed in an RC1 equipment), that the optimization – scale-up procedure previously developed allows, with a minimum calculation and experimental effort, both for a selection, at laboratory scale, of operating conditions characterized by a rapid coreactant consumption and for their safe scale-up, maximizing industrial reactor productivity.

*Keywords:* Semibatch reactors; Safe scale-up; Productivity; 4-chloro benzotrifluoride; 4-chloro, 3-nitro benzotrifluoride; Industrial process.

---

\* to whom correspondence should be addressed

## 1. Introduction

In fine chemical and pharmaceutical industry relatively fast and exothermic reactions (whose critical level with respect to runaway phenomena is usually classified through Stoessel's scale<sup>1</sup>) are typically performed in indirectly cooled semibatch reactors (SBRs), in which conversion rate can be controlled by dosing one of the reactants (called coreactant) at a sufficiently low rate so that cooling system can remove the heat evolved. Under such conditions, coreactant accumulation in the system is effectively hindered and danger of a reaction thermal loss of control is consequently minimized. Operating the process under a low coreactant accumulation is of particular importance when dealing with reaction systems -such as nitrations- which can undergo strongly exothermic and gas producing decomposition events above a threshold temperature, implying dangerous overpressurizations of the reaction vessel.

In process safety literature of the last thirty years a number of simple criteria for preventing coreactant accumulation in exothermic SBRs have been developed<sup>2-15, 33-38</sup>. These criteria can be based on thermal effects related to accumulation phenomena: actual temperature-time profile is compared with a target one, arising from low accumulation and high cooling efficiency operating conditions. On this basis different reactor thermal behaviors can be represented in a suitable dimensionless space in which a line can be identified bounding a region where excessive coreactant accumulation occurs. Such diagrams -called boundary diagrams (BDs)- allow end users for a simple selection, at laboratory scale, of sufficiently low accumulation operating conditions<sup>16-18</sup> with a minimum experimental effort, mainly consisting in a reliable kinetic characterization of the reaction system (performed through e.g. adiabatic calorimetric experiments<sup>18</sup>), which is of crucial importance for a reliable application of the method<sup>6,11,12,18</sup>.

However, the real problem to be faced when dealing with a number of exothermic semibatch processes of industrial relevance is that they can undergo undesired events above a Maximum Allowable Temperature (in the following referred to as MAT), which is typically related either to safety or selectivity constraints. Moreover, limiting accumulation phenomena can be just a

1  
2  
3 necessary but not a sufficient condition to prevent the exceeding of a threshold temperature. So the  
4  
5 usage of target temperature-time profile as a peak reaction temperature estimation can lead to the  
6  
7 selection of reactor operating conditions which may significantly lower industrial reactor  
8  
9 productivity. For these reasons Maestri and Rota<sup>6,19</sup> developed a new typology of diagrams -called  
10  
11 temperature diagrams (TDs)- which, on the basis of the same set of dimensionless parameters  
12  
13 involved in boundary diagrams, allow end users for a simple check on maximum reactor  
14  
15 temperature expected, to be compared with the experimentally determined MAT constraint.  
16  
17

18  
19 Recently, the method of boundary and temperature diagrams has been extended, by Maestri and  
20  
21 Rota<sup>20</sup>, to homogeneous SBRs which exhibit an autocatalytic behavior and, consequently, safety  
22  
23 criteria developed for non-autocatalytic reaction systems can not be applied<sup>7,13-15</sup>.  
24  
25

26  
27 Once a set of safe operating conditions for a semibatch reaction process has been identified at  
28  
29 laboratory scale, through the aforementioned criteria, selected process parameters must be then  
30  
31 safely scaled-up to full scale reactor, whose productivity must be maximized. Such a problem had  
32  
33 not been specifically faced in the existing literature through the same simple and general approach  
34  
35 as which employed for process safety analysis performed at laboratory scale. For these reasons  
36  
37 Maestri et al.<sup>2</sup> developed a simple optimization – scale-up procedure which, on the basis of  
38  
39 generalized forms of boundary and temperature diagrams (called, respectively, Inherently Safe  
40  
41 Conditions (ISC) and Temperature Rise Curve (TRC) diagrams), allows end users for safely  
42  
43 scaling-up operating conditions selected at laboratory scale to full plant scale maximizing industrial  
44  
45 reactor productivity.  
46  
47

48  
49 In this work such a procedure is applied to the analysis of a nitration process performed in the  
50  
51 agrochemical industry, that is the nitration, through mixed acids, of 4-chloro benzotrifluoride (in the  
52  
53 following referred to as 4-chloro BTF) to 4-chloro, 3-nitro benzotrifluoride (in the following  
54  
55 referred to as 4-chloro, 3-nitro BTF) for the synthesis of 2,6-dinitro, 4-trifluoromethyl  
56  
57 dialkylanilines, widely employed as herbicides. The reaction in question corresponds to the top  
58  
59 level in Stoessel's classification of runaway reactions<sup>1</sup>, for which synthesis reaction thermal loss of  
60

1  
2  
3 control implies the triggering of dangerous decompositions of reaction mass, without any tempering  
4  
5 effect due to solvent evaporation.  
6  
7

8 After preliminary DSC characterizations of the involved chemical species, thermal stability of  
9  
10 reaction mass has been investigated through adiabatic calorimetric experiments. Then, microkinetic  
11  
12 parameters have been estimated through reaction calorimetry experiments performed under  
13  
14 kinetically controlled conditions. The general optimization – scale-up procedure developed in the  
15  
16 first part of this work<sup>2</sup> has been, then, applied both to the selection of safe operating conditions at  
17  
18 laboratory scale (obtaining a good agreement with experimental results) and to the optimum scale-  
19  
20 up (for what concerns industrial reactor productivity) of the selected set of process parameters.  
21  
22 Identified scaled-up conditions have been found to be consistent with results of more detailed  
23  
24 mathematical modeling.  
25  
26  
27

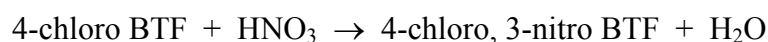
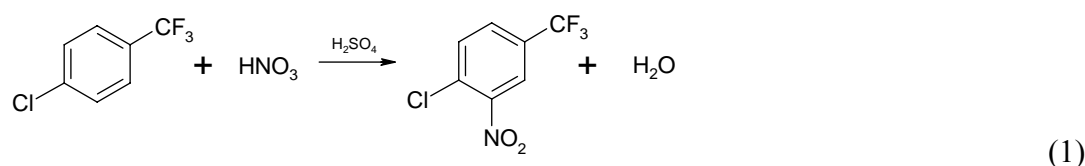
## 28 29 **2. Reaction system**

30  
31 Many issues about aromatic nitrations in mixed acids remain without exhaustive responses, despite  
32  
33 the fact that nitrations were among the earliest processes to be operative on large scale when heavy  
34  
35 organic chemical industry developed at the beginning of the last century<sup>17</sup>. The dynamic behavior of  
36  
37 an aromatic nitration in mixed acids involves a number of problems related to simultaneous  
38  
39 interphase and intraphase mass transfer phenomena (if the synthesis is carried out with reactants in  
40  
41 stoichiometric quantities)<sup>21,22</sup>. These phenomena lead to complex problems during characterization  
42  
43 and scale-up of such processes, mainly arising from the interdependence among fluid properties  
44  
45 (e.g., viscosities, densities, interfacial surface properties, diffusion coefficients and distribution  
46  
47 coefficients among the phases), operating conditions (temperatures) and equipment characteristics  
48  
49 (e.g., impeller kind and size, reactor geometry)<sup>22-24</sup>, such as those ones related to phase inversion<sup>25</sup>  
50  
51 and agitator speed<sup>26</sup>. Since for the system investigated in this work one of the inorganic acids  
52  
53 (namely, the sulphuric one) acts also as a solvent and it is present in large excess, the first problem  
54  
55 can be avoided by feeding the reactor with mixed acids as initial reactant. The second one strongly  
56  
57 influences heat and mass transfer efficiencies so, in order to operate under kinetically controlled  
58  
59  
60

1  
2  
3 regime (where no heat or mass transfer limitations lower the overall conversion of the process), it is  
4  
5 necessary to work with agitator speed sufficiently high. Above a certain speed value, no more  
6  
7 effects of heat and mass transfer limitations on heat reactor flux are observed. In such conditions a  
8  
9 perfectly macromixed reaction mass is formed, no phase separation effects should occur and the  
10  
11 characteristic time of mass and heat transfer phenomena is much lower than that characteristic of  
12  
13 the reaction. However, aromatic nitrations develop high heat of reaction and are often accompanied  
14  
15 by undesirable reactions which have produced a considerable number of accidents<sup>27, 29</sup>. Therefore, a  
16  
17 deep understanding of this kind of problems is very important to design and operate safely nitration  
18  
19 plants.  
20  
21  
22  
23

24  
25 In fine chemical and pharma industry, aromatic nitrations are normally carried out in indirectly  
26  
27 cooled SBRs with intensive stirring, in order to achieve high heat and mass transfer efficiencies. In  
28  
29 the present case, the species to be nitrated (that is, 4-chloro BTF) is added to a mixture of sulfuric  
30  
31 and nitric acid in which sulfuric acid acts both as a solvent and as a dehydrating agent vs. nitric acid  
32  
33 to form the nitronium ion,  $\text{NO}_2^+$ , which is the electrophilic species reacting with the aromatic ring.  
34  
35

36 The overall reaction, taking place in the continuous acid phase, is:



47  
48 In absence of transfer limitations, reaction rate of (1) equals the overall conversion rate of the  
49  
50 aromatic species to the nitrocompound (limiting step)<sup>17</sup>.

51  
52 Conversely, the macrokinetic of the process would be controlled by one of the following steps<sup>16,17</sup>:

- 53  
54  
55  
56  
57  
58  
59  
60
- intraphase diffusion of the aromatic compound from the bulk of the organic phase to the interface: diffusion through the first boundary layer;
  - interphase diffusion of the aromatic compounds at the interface;

- intraphase diffusion of the aromatic compound from the interface to the bulk of the aqueous phase;
- diffusion of the nitro derivative compound towards the organic phase.

In this work the system analyzed has been considered as an heterogeneous (liquid-liquid) system operating in the slow reaction regime, which is known to be the most hazardous one.

### 3. Safety analysis

In the first part of this work<sup>2</sup>, a simple and general optimization – scale-up procedure for exothermic SBRs, operating under Quick onset-Fair conversion-Smooth temperature profile (QFS) conditions<sup>8</sup>, has been developed. Such a procedure allows end users for an easy selection of reactor operating conditions implying both a sufficiently low coreactant accumulation and a peak reaction temperature lower than a threshold value (MAT), typically arising either from safety or selectivity constraints.

The use of such a procedure is based on two different typologies of diagram: Temperature Rise Curve diagrams (TRC) and Inherently Safe Conditions diagrams (ISC). The first ones are a generalized form of temperature diagrams, generated in the same space, dimensionless temperature rise,  $\Psi$ , vs. exothermicity number,  $E_x$ , and accounting for the maximum allowable temperature for the analyzed process. The second ones are a simplified form of boundary diagrams (reactivity number,  $R_{y,QFS}$ , vs. cooling number,  $Co$ ) providing a safe check on coreactant accumulation. The most important dimensionless parameters appearing in such diagrams are: an exothermicity number,  $E_x$ , related to reaction enthalpy, and a reactivity number,  $R_y$ , depending on initial sensitivity of reaction rate with respect to temperature.

For the reaction system in question exothermicity number is equal to:

$$E_x = \frac{E}{RT_{cool}^2} \frac{\Delta T_{ad,0}}{\varepsilon(CO + R_H)} \quad (2)$$

whereas reactivity number (for reactions orders equal to 1 for both the reactants) can be computed through the following expressions, under kinetically (equation 3) or diffusion (equation 4) controlled operating conditions respectively:

$$R_y = \frac{k|_{T_0} \cdot t_D C_{HNO_3,0} m_{4-chloroBTF}}{\varepsilon(Co + R_H)} \quad (3)$$

$$R_y = \frac{k^{1/2}|_{T_0} \cdot t_D C^{1/2}_{HNO_3,0} m_{4-chloroBTF} \cdot 6/d_{b,0} D_{4-chloroBTF}^{1/2}}{\varepsilon(Co + R_H)} \quad (4)$$

A determined set of reactor operating conditions (individuated by  $E_x$  and  $R_y$  calculation) can be adopted if both the following constraints are fulfilled:

- reactivity number,  $R_y$ , higher than a threshold value,  $R_{y,QFS}$ , evaluated, at the current cooling number,  $Co$ , through the graphical correlation provided by the Inherently Safe Conditions diagram (ISC) of Figure 1;
- maximum peak reaction temperature, as estimated through the general temperature rise curve (TRC) represented in Figure 2 sufficiently lower than MAT.

#### **4. Experimental Techniques and Procedures**

In this section all the employed experimental techniques and procedures are briefly summarized.

##### *4.1 Differential Scanning Calorimetry (DSC)*

This calorimetric technique allows for reagents and products thermochemical characterization by comparing the thermal behavior of a sample with that of a reference.

Particularly, sample and reference are heating increasing their temperature at constant rate: whenever a chemical (and/or a physical) process occurs into the sample, the heat released or absorbed (according to the fact that a process could be exothermic or endothermic) will tend to increase or decrease sample temperature. The result is a temperature difference between sample and reference. The instrument task is to balance this temperature difference with an appropriate electrical power which regulates reference temperature. The evaluation of this electrical power is a direct measure of the energy dues to transformation occurred in the sample. In this way, the



1  
2  
3 instrument is able to record the rate at which the sample develops or absorbs heat ( $dQ/dt$ ) during the  
4 transformation and to generate characteristic diagrams which report heat power exchanged between  
5 sample and reference versus temperature ( $dQ/dt$  vs T) or time ( $dQ/dt$  vs t). These diagrams show the  
6 number and the characteristics of all thermal effects, the temperatures (or time) at which these  
7 effects take place and, finally, the importance of these ones (the pick area of diagram  $dQ/dt$  vs time  
8 is proportional to the energy associated to the transformation).  
9

10 All DSC tests performed in this work has been carried out using a sample heating rate of 10 °C/min  
11 and medium pressure viton/120  $\mu$ L sample holders. The investigated temperature range has been 30  
12 – 280 °C.  
13  
14

#### 15 4.2 Accelerating Rate Calorimeter (ARC)

16  
17 ARC, produced by the Columbia Scientific Instruments, is an adiabatic calorimeter controlled by a  
18 microprocessor and a data system of analysis particularly suitable to study homogeneous reacting  
19 systems subject to decomposition. It is composed by the following items: a spherical sample holder,  
20 built of Hastelloy C and placed in an insulated vessel; a radiant heater, which rises sample  
21 temperature up to a fixed value; a thermocouple fixed to the sample holder wall and employed to  
22 record sample temperature; an insulated covering (jacket) with three thermocouples and eight  
23 heaters (this configuration guarantees to heat up the oven with the same rate as the sample holder  
24 during an exothermic reaction); a capillary tube which links sample holder to a pressure transducer.  
25

26 Two different typologies of experiments can be performed by ARC:

- 27 - “iso-aging” test: the instrument keeps the sample in isothermal conditions until an exothermic  
28 effect is detected, then the test continues in adiabatic mode;
- 29 - dynamic standard “HEAT” – “WAIT” – “SEARCH” (HWS) test: the sample is warmed up  
30 (“HEAT”) by a radiant heater at a desired temperature, then the instrument wait (“WAIT”) until all  
31 temperatures are stabilized and, finally, it starts to search for exothermic effects (“SEARCH”),  
32 namely a self heating rate of reaction mass into the sample larger than 0.02 °C/min. This research  
33 terminates either when a predetermined time is passed (10 min) or a sample self heating rate which  
34

1  
2  
3 exceeds 0.02 °C/min is detected. If an exothermic reaction is revealed, the instrument collects  
4  
5 automatically temperature and pressure data in function of time, shifting to adiabatic mode until the  
6  
7 reaction ends (self-heating rate lower than the fixed limit). If an exothermic reaction is not revealed  
8  
9 a new sequence of HWS is started at higher temperature. From a single ARC test it is possible to  
10  
11 obtain several information, such as: initial and end temperature of any detected exothermic effects;  
12  
13 sample self-heating rate at any temperature; adiabatic temperature increase; pressure at any  
14  
15 temperature; pressure increase rate.  
16  
17  
18

19  
20 Results obtained are strictly dependent by sample holder thermal inertia,  $\Phi$ . Consequently,  
21  
22 experimental data have to be corrected to take into account this effect.  
23

24  
25 Temperature and pressure operative ranges between the different test typologies may be conducted  
26  
27 varying from 25 to 500 °C and from 1 to 170 bar.  
28

#### 29 *4.3 Reaction calorimeter (RC1)*

30  
31 This calorimeter is a laboratory reactor of 1.2 liters capacity, equipped with an external jacket to  
32  
33 heat or cool the reaction mass. Instruments are controlled by a software which allows to obtain,  
34  
35 through calibration procedures, chemical and physical system properties of interest. The calorimeter  
36  
37 may operate in three different modes:  
38  
39

- 40 - T<sub>j</sub>-mode: calorimeter controls jacket temperature;
- 41  
42 - T<sub>r</sub>-mode: calorimeter controls reactor temperature;
- 43  
44 - Adiabatic mode: calorimeter controls the difference between jacket and reactor temperature.  
45  
46  
47

48  
49 In this work, RC1 has been used in two different modes: adiabatic (to find microkinetic rate  
50  
51 expression) and T<sub>j</sub>-mode (to simulate the system behaviour in isoperibolic conditions).  
52

53  
54 To heat or cool the reaction mass, through a proportional or integral-proportional controller,  
55  
56 calorimeter mixes two silicon oils at two different temperatures (low temperature oil and high  
57  
58 temperature oil); this “oils mixture” is sent to the reactor jacket. Low temperature oil is obtained by  
59  
60 a cryostat circuit and high temperature oil is obtained by an electrical resistance of 2 kW.

1  
2  
3 Calorimeter is equipped with a thermocouple and a calibration probe, which is necessary in order to  
4  
5 determine the global heat transfer coefficient.  
6  
7

## 8 **5. Optimization – scale-up procedure**

9  
10 In order to identify safe and productive operating conditions, with a minimum experimental effort,  
11  
12 the optimization – scale-up procedure, discussed in the first part of this work<sup>2</sup>, has been used as  
13  
14 summarized in the following five steps.  
15  
16

### 17 *5.1 Calorimetric screening tests*

18  
19 Nitrocompounds incorporate in their chemical structure both an oxidizing group and an organic  
20  
21 substrate which may be oxidized. It is therefore crucial to perform a preliminary investigation of the  
22  
23 thermal stability of species and mixtures involved in the process. Such an analysis can be carried  
24  
25 out first theoretically (that is, through suitable softwares such as the CHETAH package of ASTM<sup>32</sup>)  
26  
27 and then experimentally (through e.g. DSC measurements).  
28  
29

30  
31 For what concern theoretical analysis, the aforementioned CHETAH software of ASTM has been  
32  
33 used to estimate relative thermal stability of aromatic reactants and products. Even if CHETAH is a  
34  
35 gas phase thermodynamic estimation tool it provides reasonably results about thermal stability of  
36  
37 liquid species. CHETAH, through combination of a number of criteria involving heat of  
38  
39 decomposition, heat of combustion and oxygen stoichiometric balance for molecules, assigns to  
40  
41 each chemical species an energy release potential (ERP): the lower the ERP value is, the higher the  
42  
43 thermal instability of substance is. In the present case, a lower ERP value for 4-chloro, 3-nitro BTF  
44  
45 (-0.548 – High instability) than for 4-chloro BTF (0.314 – Low instability) has been calculated,  
46  
47 hence confirming an expected lower thermal stability of nitrocompound.  
48  
49  
50  
51

52  
53 DSC standard tests have been performed on 4-chloro BTF and its nitroderivative and they are  
54  
55 reported in Figure 3 for static air and nitrogen, respectively. It can be observed that both the  
56  
57 substances are stable in static air (no oxidative phenomena occur) and in nitrogen in all the explored  
58  
59 temperature range. However, since thermal stability of nitrocomponunds can be greatly influenced  
60

1  
2  
3 by a number of chemical species (in particular by sulfuric acid, even in traces<sup>27, 29</sup>), it is crucial to  
4 perform a thermal stability characterization also of the actual reaction mixture.  
5  
6

7  
8 Consequently, reacting mixture stability has been analyzed through a standard HWS test in an ARC  
9 equipment. Average reaction mass heat capacity (equal to 1.35 kJ/(kg K)) and reaction enthalpy  
10 (equal to 150.1 kJ/mol) have been preliminary determined by calibration in an RC1 equipment.  
11  
12

13  
14 Figure 4 shows temperature and pressure profiles measured in the ARC experiment. Two  
15 exothermic effects can be recognized: the first one, occurring at 80°C, is related to a partial  
16 dinitration of the product (due to the slight nitric acid excess under which the synthesis is carried  
17 out) and it is characterized, under the operating conditions of the test, by an adiabatic temperature  
18 rise of only 5°C; the second one, occurring at 141°C, is strongly exothermic and implies a huge  
19 pressure increase due to the decomposition of reaction mass with production of permanent gases. It  
20 can be concluded that a decomposition of final reacting mixture is detected at 141°C: this  
21 phenomenon had not been detected for pure species thus confirming, once more, that thermal  
22 instability of a reaction product can be enhanced by other components present into the reacting  
23 mixture and, when dealing with nitration processes carried out in mixed acids, by sulfuric and nitric  
24 acid<sup>27, 29</sup>.  
25  
26  
27  
28  
29  
30  
31  
32  
33  
34  
35  
36  
37  
38  
39  
40

41 In Table 1 the main parameters computed from the ARC experiment results are reported. These  
42 values have been corrected according to the calorimeter thermal inertia, as summarized in a value of  
43 the  $\Phi$  factor, which is the ratio of the sum of sample and calorimeter heat capacity with respect to  
44 sample heat capacity.  
45  
46  
47  
48  
49

50  
51 On the basis of detected decomposition temperature (which is equal to 141°C) and solvent boiling  
52 point (which, for sulfuric acid, is equal to 290°C) it can be concluded that the reaction in question  
53 belongs to the top level of Stoessel's classification of runaway reactions<sup>1</sup>, for which reaction  
54 thermal loss of control can lead to the triggering of a decomposition event without any tempering  
55 effect due to the solvent evaporation.  
56  
57  
58  
59  
60

## 5.2 Adiabatic Reaction Calorimetry

Microkinetic parameters of 4-Cl BTF nitration reaction have been estimated through adiabatic calorimetric experiments in an RC1 equipment.

First of all some preliminary tests have been performed in an ARC calorimeter (which is equipped with a magnetic stirrer mostly suitable for homogeneous solutions<sup>27, 29</sup>), at different agitator speed, by one shot dosing of 4-Cl BTF on mixed acids. Since such experiments showed that, changing the stirring rate from 100 up to 500 rpm results change, as can be seen by Figure 5, an adiabatic test for estimating microkinetic parameters has been performed in an RC1 calorimeter, where a much larger stirring efficiency is achievable.

Calibration tests carried out with the initial and final reaction mixtures led to an average value of the overall heat transfer coefficient equal to 110W/(m<sup>2</sup> K). The adiabatic experiment has been carried out loading into the calorimeter 149g of a 4:1 by weight ratio mixture of sulfuric to nitric acid, further diluted with 830g of 98% wt. sulfuric acid in order to limit the adiabatic temperature rise by 40°C for safety reasons. 80.8g of 4-chloro BTF have been then dosed over a 2s period and at a stirring speed equal to 500rpm. The temperature vs. time experimental data have been then fitted through BatchCAD® process simulation software in which a detailed mathematical model of the reaction system was previously set. The best fit of experimental temperature vs. time data has been obtained for the set of microkinetic parameters resulting in the following rate of reaction expression:

$$r = k \cdot C_{4\text{-chloroBTF},c} \cdot C_{\text{HNO}_3,c} \quad (5)$$

where  $k = 3.228 \cdot 10^{12} \exp(-87260/RT)$  is the rate constant of reaction (1) and the units are kJ, kmol, K, m<sup>3</sup>, s. A comparison between experimental and fitted data is shown in Figure 6.

Finally, when dealing with an heterogeneous (liquid-liquid) system, a theoretical control on Hatta, Ha, and Hinterland, Al, number values must be performed in order to establish if the system operates under kinetically controlled, or slow, regime (that is, with a negligible influence of interphase mass transfer phenomena on the overall conversion rate). In particular slow reaction

regime is characterized by  $Ha < 0.3$  and  $Al \times Ha^2 \ll 1^{28}$ . In our cases, at the beginning of the synthesis,  $Ha = 0.2$  and  $Al \times Ha^2 = 0.01$ , hence confirming that the process operates under slow reaction regime since the beginning of the synthesis.

### 5.3 Optimum dosing time at laboratory scale

Knowing process recipe and fixing initial reactor temperature,  $T_0$ , at 310 K (since reaction product can undergo a further nitration, initial reaction temperatures, when nitric acid concentration is still high, must not exceed 40°C) TRC and ISC diagrams can be used to identify safe and productive operating conditions at the RC1 scale. As a first step an effective MAT value (EMAT), suitably lower than MAT value measured by the ARC test, must be selected for safety reasons. In this work a 0.05 safety factor, *toll*, has been used, leading to  $EMAT = 393$  K which corresponds to  $\Psi_{EMAT} = 1.27$ . From this value, TRC diagram (see Figure 2) gives a corresponding maximum acceptable value of exothermicity number,  $E_{x,EMAX}$ , which is equal to 8.2.

Then, from  $E_{x,EMAX}$  expression it is possible to determine a minimum cooling number ( $Co_{MIN} = \gamma \Delta \tau_{ad,0} / \tau_0^2 \varepsilon E_{x,EMAX} - R_H$ ) equal to 4.5 and, finally, a minimum dosing time ( $t_{D,MIN,RC1} = Co_{MIN} \tilde{\rho}_c \tilde{C}_{P,c} V_c \varepsilon / (UA)_0$ ) equal to 636 s (about 10 min). From this calculated  $t_{D,MIN,RC1}$  value it is possible to evaluate a system reactivity number,  $R_{y,RC1}$ , equal to 0.0623 which is larger than the correspondent  $R_{y,QFS}$  value, evaluated at  $Co_{MIN} = 4.5$ , on ISC diagram (which is equal to 0.0550, see Figure 1). All the operative parameters are summarized in Table 2.

### 5.4 Isoperibolic RC1 test

The operating conditions previously calculated must be validated by an RC1 test to verify if the process operates under low coreactant accumulation conditions and with a maximum reactor temperature lower than EMAT. Therefore, an RC1 isoperibolic test has been performed using as dosing time that one calculated by the optimization procedure (namely,  $t_D \sim 11$  min). Figure 7 shows a good agreement between experimental and predicted dimensionless temperature profiles; this confirms the reliability of the previously estimated thermo-kinetic parameters. From Figure 7 it is

1  
2  
3 also possible to determine the maximum reactor temperature during synthesis run equal to 1.22,  
4  
5 which is lower than the correspondent  $\psi_{EMAT} = 1.27$ ; this confirms the reliability of the TRC  
6  
7 diagrams. Calorimetric conversion at the end of the dosing period has been calculated equal to  
8  
9 about 98%. This confirms that the reaction is almost finished at the end of the dosing period and no  
10  
11 coreactant accumulation occurs, thus supporting the reliability of the ISC diagram.  
12  
13

### 14 15 *5.5 Scale-up procedure*

16  
17 The optimum operating conditions at laboratory scale must be then safely scaled-up to the industrial  
18  
19 reactor maximizing process productivity. In this work, an effectively stirred  $9\text{m}^3$  tank reactor  
20  
21 equipped with a  $45\text{m}^2$  overall heat transfer surface and operating in the kinetically controlled regime  
22  
23 (as confirmed by the values of both  $Ha=0.2$  and  $Al \times Ha^2 = 0.02$  at the beginning of the synthesis,  
24  
25 which confirm that the process operates under slow reaction regime) has been considered, whose  
26  
27 main parameters are summarized in Table 3.  
28  
29

30  
31 From the previously calculated  $\psi_{EMAT} = 1.27$  and through the general temperature rise correlation  
32  
33 represented in Figure 2, the same previous values of  $E_{x,EMAX} = 8.2$  and  $C_{O,MIN} = 4.5$  can be obtained.  
34  
35

36  
37 From data reported in Table 3 the value of  $t_{D,MIN,ind} \sim 66$  min can be easily computed. This value is  
38  
39 consistent with that identified through time consuming trial and error computations carried out with  
40  
41 standard process simulation softwares, such as BatchCad®.  
42

43  
44 It should be noted that, while at laboratory scale the maximum temperature value estimated from  
45  
46 the initial target temperature is lower than that given by TRC and, consequently, initial target  
47  
48 temperature value could be used for estimating peak temperature, the opposite is true at industrial  
49  
50 scale where initial target temperature would provide a useless overestimation of the peak  
51  
52 temperature. It is interesting to note that similar, but less conservative, conclusions can be achieved  
53  
54 by an order of magnitude estimation using standard correlations. Since the procedure requires  
55  
56 cooling numbers at RC1 and industrial scales being equal and considering that they are roughly  
57  
58 related to each other as follows:  
59  
60

$$Co_{RC1} = const \left( \frac{U \cdot t_D}{D} \right)_{RC1} \quad (6)$$

$$Co_{ind} = const \left( \frac{U \cdot t_D}{D} \right)_{ind}$$

if  $Co_{RC1} = Co_{ind}$ , the ratio of industrial to laboratory dosing time is roughly proportional to the product of two factors:

$$\frac{t_{D,ind}}{t_{D,RC1}} = \frac{D_{ind}}{D_{RC1}} \cdot \frac{U_{RC1}}{U_{ind}} \quad (7)$$

The first one (which is the ratio of industrial to laboratory reaction vessel characteristic dimension) is always much higher than one and, mostly, implies dosing time increase when moving from laboratory to industrial scale. In the present case, being RC1 calorimeter and industrial reactor diameters equal to about 10 cm and 2 m respectively, such a factor is equal to about 20.

The second one (which is the ratio of laboratory to industrial effective overall heat transfer coefficients) decreases as industrial reactor cooling efficiency increases: such a behavior is logical, since a high reactor cooling efficiency (which is typical of reactors in which nitration with mixed acids are performed) allows for a lower dosing time. This factor can be estimated through standard correlation<sup>30</sup> such as:  $U_{RC1}/U_{ind} = (L_{RC1}/L_{ind})^{1/3} (N_{RC1}/N_{ind})$ , L and N being the blade width and the stirring speed respectively. Moreover, since the reactor is equipped with a jacket and a coil while RC1 with a jacket only the factor must be divided by  $(1 + A_{coil}/A_{jacket})_0$ , which is equal to about 3.5.

Approximating the ratio between the blade lengths at the two scales to that between the vessel characteristic dimension it follows  $U_{RC1}/U_{ind} \approx (0.1m/2m)^{1/3} (500rpm/200rpm) \approx 0.25$ .

From these considerations, an increased of a factor equal to about 5 is expected in dosing time when moving from laboratory to full plant scale, which is of the same order of magnitude of the 66 min/11 min = 6 value obtained by the procedure.



1  
2  
3 Through ISC of Figure 1 it can be easily verified that the scaled-up conditions are characterized by  
4 an  $R_y$  value (which can be computed from the data reported in Table 3) equal to about 0.4 which is  
5 much higher than the  $R_{y,QFS}$  parameter at the current  $Co$  value.  
6  
7  
8  
9

## 10 **6. Sensitivity analysis**

11  
12 Optimization – scale-up procedure needs of a series of experimental parameters inevitably subjected  
13 to uncertainty. In order to define *how safe* are the industrial reactor operating conditions arising  
14 from such a procedure, it is necessary to perform a sensitivity analysis with respect to the  
15 parameters subjected to some uncertainty<sup>31</sup>. The straightest way to execute such an analysis is to  
16 perform a numerical sensitivity analysis. However, in the first part of this work, easy checks for  
17 heterogeneous kinetically controlled systems have been also developed, resulting in the relations  
18 reported in Table 4 and 5. Therefore, using such relations together with the data summarized in  
19 Table 3, it is possible to perform an analysis aimed to establish *how safe* are the operating  
20 conditions selected through the optimization – scale-up procedure considered. The results are  
21 reported in same Table 5.  
22  
23  
24  
25  
26  
27  
28  
29  
30  
31  
32  
33  
34  
35

36 As it can be easily observed from Table 5, all checks are positive when assuming a 5% uncertainty  
37 on all the parameters of this analysis. This demonstrates that the optimization – scale-up procedure  
38 developed is able to provide safe operating conditions without penalized process productivity.  
39 However, it should be stressed that this conclusion relies on the assumed value for the uncertainty,  
40 which is 5%. Larger uncertainty could lead to possible unsafe conditions, with particular regards to  
41 the activation energy ( $\gamma$ ). In our case assuming a 10% uncertainty on all parameters but  $\gamma$  leads to  
42 safe operating conditions because all checks reported in Table 5 are still satisfied. For what  
43 concerns  $\gamma$  it has been found that uncertainties higher than 5.5% can not be accepted because it  
44 could imply hazardous operating conditions.  
45  
46  
47  
48  
49  
50  
51  
52  
53  
54  
55  
56  
57  
58  
59  
60

## 7. Conclusions

Nitration of 4-chloro BTF to 4-chloro, 3-nitro BTF carried out in indirectly cooled liquid-liquid SBRs has been analyzed both experimentally through calorimetric techniques and theoretically through the general optimization - scale-up procedure presented in the first part of this work<sup>2</sup>.

After a preliminary investigation about thermal stability of the involved chemical species and mixtures, performed through DSC and ARC experiments respectively, reaction microkinetic parameters have been derived through RC1 experiments.

In order to select at the laboratory scale through a minimum experimental and calculation effort operating conditions implying both a sufficiently low 4-chloro BTF accumulation in the system and peak reaction temperatures lower than a threshold value, the aforementioned procedure has been used, whose predictions have been found to be consistent with experimental results.

The same procedure has been finally used to show how to perform a safe scale-up of the selected set of reactor operating parameters to the industrial scale, maximizing industrial reactor productivity.

Finally, to estimate *how safe* the procedure developed is, a sensitivity analysis on the experimental parameters subjected to uncertainty has been carried out, showing that all safety checks was positive. Optimization – scale-up procedure developed is, consequently, safe even when the experimentally determined parameters range in a given error interval (say +/- 5%).

Finally, it should be mentioned that in the case of aromatic nitrations many other aspects should be carefully considered. Among the others, the possibility of starting the reaction in the fast regime and to finish it in the slow one due to the water produced by the reaction<sup>21-23</sup>; phase inversion which could change the controlling mechanism<sup>25</sup> and stirring aspects, which could lead to runaway in scaled-up conditions<sup>26</sup>.

**Nomenclature**

<i>a</i>	volumetric specific intraphase surface, 1/m
A	heat transfer area of the reactor (associated to the jacket and/or the coil), m <sup>2</sup>
Al	Hinterland ratio, - $Al = (1 - \varepsilon)k_{4-Cl-BTF_{phs}}^{(L)} / aD_{4-Cl-BTF}^{(L)}$
ARC	Accelerated Rate Calorimeter
BD	Boundary Diagram
C	molar concentration, kmol/m <sup>3</sup>
4-chloro BTF	4-chloro benzotrifluoride, reactant in reaction (1)
4-chloro, 3-nitro	4-chloro, 3-nitro benzotrifluoride, product of reaction (1)
BTF	
const	constant value, -
Co	$= (UA)_0 t_D / (\tilde{\rho}_c \tilde{C}_{p,c} V_D)$ , cooling number, -
$\tilde{C}_p$	molar heat capacity, kJ/(kmol·K)
$\hat{C}_p$	massive heat capacity, kJ/(kg·K)
$d_{b,0}$	drop diameter when hold up of the dispersed phase approaching zero, m
D	reaction vessel diameter, m
D <sup>(L)</sup>	Diffusivity in liquid phase, m <sup>2</sup> /s
Da	$= kt_D C_{HNO_3,0}$ , Damköhler number, -
dQ/dt	heat power released or absorbed in a DSC test
DSC	Differential Scanning Calorimetry
E	activation energy, kJ/kmol
EMAT	$= MAT(1-toll)$ , effective maximum allowable temperature, -
ERP	energy release potential, -
E <sub>x</sub>	exothermicity number, eq. (2), -

1		
2		
3	$\Delta\tilde{H}$	reaction enthalpy, kJ/kmol
4		
5	Ha	Hatta number, - $Ha = \sqrt{kC_{HNO_3}D_{4-Cl-BTF}^{(L)}} / k_{4-Cl\_BTF_{phs}}^{(L)}$
6		
7		
8	HNO <sub>3</sub>	Nitric Acid, reactant of reaction (1)
9		
10	H <sub>2</sub> SO <sub>4</sub>	Sulfuric Acid, catalyst
11		
12	H <sub>2</sub> O	Water, product of reaction (1)
13		
14	ISC	Inherently Safe Condition Diagram
15		
16	$k_{4-Cl-BTF,phs}^{(L)}$	overall mass transfer coefficient, m/s
17		
18	k	microkinetic constant, m <sup>3</sup> /(kmol s)
19		
20	L	Blade width, m
21		
22	m	Mass, kg
23		
24	m	equilibrium distribution coefficient ( $m_{4-chloro\ BTF} = C_{4-chloro\ BTF,c} / C_{4-chloro\ BTF,d}$ ), -
25		
26	m	reaction order with respect to HNO <sub>3</sub> , -
27		
28	MAT	Maximum allowable temperature, °C or K
29		
30	MTSR	Maximum temperature achievable by the synthesis reaction, °C or K
31		
32	n	reaction order with respect to 4-Cl-BTF, -
33		
34	N	stirring speed, rpm
35		
36	NO <sub>2</sub> <sup>+</sup>	Nitronium ion
37		
38	PID	Proportional – Integral – Derivative controller
39		
40	QFS	Quick onset-Fair conversion-Smooth temperature profile
41		
42	R	reaction rate referred to the total liquid volume, kmol/(m <sup>3</sup> ·s)
43		
44	R	gas constant = 8.314, kJ/(kmol·K)
45		
46	RC1	Reaction Calorimeter
47		
48	R <sub>H</sub>	heat capacity ratio, -
49		
50	R <sub>y</sub>	reactivity number, eqs. (3) and (4), -
51		
52	SBR	Semi-Batch Reactor
53		
54		
55		
56		
57		
58		
59		
60		

1		
2		
3	t	time, s
4		
5	T	temperature, K
6		
7	TD	Temperature Diagram
8		
9		
10	<i>Toll</i>	safety parameter for MAT value: $EMAT = (1-toll) MAT$
11		
12	TRC	Temperature Rise Curve Diagram
13		
14		
15	$T_{rif}$	Reference temperature, equal to 300 K
16		
17		
18	$\Delta T_{ad,0}$	$= \frac{(-\Delta\tilde{H})C_{HNO_3,0}}{\tilde{\rho}_c \tilde{C}_{P,c}}$ , adiabatic temperature rise, °C or K
19		
20		
21		
22	U	specific overall heat transfer coefficient, kW/(m <sup>2</sup> K)
23		
24	(UA) <sub>0</sub>	overall heat transfer coefficient at initial conditions, kW/K
25		
26		
27	V	volume, m <sup>3</sup>
28		
29		
30		

### *Subscripts and superscripts*

31		
32		
33		
34	Ad	Adiabatic
35		
36	c	continuous phase
37		
38	4-chloro BTF	4-chloro benzotrifluoride
39		
40		
41	4-chloro, 3-nitro BTF	4-chloro, 3-nitro benzotrifluoride
42		
43	Coil	Coil
44		
45		
46	Cool	Coolant
47		
48	d	dispersed phase
49		
50		
51	D	dosing stream or dosing time
52		
53	EMAT	evaluated at the effective maximum allowable temperature (EMAT)
54		
55	EMAX	maximum in correspondence of the effective maximum allowable
56		
57		
58		temperature (EMAT), in $E_{x,EMAX}$
59		
60	HNO <sub>3</sub>	nitric acid

1		
2		
3	Ind	at the industrial scale
4		
5	Jacket	Jacket
6		
7		
8	MAT	at the maximum allowable temperature
9		
10	MIN	Minimum, in $E_{x,MIN}$
11		
12	QFS	in correspondence of QFS conditions, in $R_{y,QFS}$
13		
14		
15	RC1	at the RC1 scale
16		
17	$  T_0$	evaluated at initial system temperature
18		
19	X	in the exothermicity number $E_x$
20		
21	Y	in the reactivity number $R_y$
22		
23		
24	0	start of the dosing period
25		
26		
27		
28		

*Greek symbols*

29		
30		
31	$\gamma$	= $E/(RT)$ , dimensionless activation energy for reaction (1), -
32		
33	$\varepsilon$	relative volume increase at the end of the semibatch period, -
34		
35	$\varepsilon$	relative error in sensitivity analysis
36		
37	$\vartheta$	= $t/t_D$ , dimensionless time, -
38		
39	$\tilde{\rho}$	Molar density, $\text{kmol/m}^3$
40		
41	$\tau$	= $T/T_{rif}$ , dimensionless temperature, -
42		
43	$\Delta\tau_{ad,0}$	= $\frac{(-\Delta\tilde{H})C_{HNO_3,0}}{\tilde{\rho}_c\tilde{C}_{p,c}T_{rif}}$ , dimensionless adiabatic temperature rise, -
44		
45	$\Phi$	= $\left[ (m\hat{C}_p)_{sample} + (m\hat{C}_p)_{calorimeter} \right] / (m\hat{C}_p)_{sample}$ , thermal inertia factor, -
46		
47	$\Psi$	= $(T_{max}/T_0)_{max}$ , maximum dimensionless temperature rise, -
48		
49		
50		
51		
52		
53		
54		
55		
56		
57		
58		
59		
60		

**Literature cited**

- (1) Stoessel, F. What is Your Thermal Risk. *Chem. Eng. Prog.* **1993**, *10*, 68.
- (2) Maestri, F.; Copelli, S.; Rota, R.; Lunghi, A.; Gigante, L.; Cardillo, P. A Simple Procedure for Optimal Scale-up of Fine Chemical Processes. Part I: Practical Tools. *Ind. Eng. Chem. Res.*, in press.
- (3) Hugo, P.; Steinbach, J. Praxisorientierte Darstellung der Thermischen Sicherheitsgrenzen für den Indirekt Gekühlten Semibatch-Reaktor. *Chem. Eng. Technol.* **1985**, *57*, 780.
- (4) Hugo, P.; Steinbach, J. A Comparison of the Limits of Safe Operation of a SBR and a CSTR. *Chem. Eng. Sci.* **1986**, *41*, 1081.
- (5) Hugo, P.; Steinbach, J.; Stoessel, F. Calculation of the Maximum Temperature in Stirred Tank Reactors in Case of a Breakdown of Cooling. *Chem. Eng. Sci.* **1988**, *43*, 2147.
- (6) Maestri, F.; Rota, R. Safe and Productive Operation of Homogeneous Semibatch Reactors. I: Development of a General Procedure. *Ind. Eng. Chem. Res.* **2006**, *45*, 8002.
- (7) Molga, E. J.; Lewak, M.; Westerterp, K. R. Runaway Prevention in Liquid-Phase Homogeneous Semibatch Reactors. *Chem. Eng. Sci.* **2007**, *62*, 5074.
- (8) Steensma, M.; Westerterp, K. R. Thermally Safe Operation of a Cooled Semibatch Reactor. Slow Liquid-Liquid Reactions. *Chem. Eng. Sci.* **1988**, *43*, 2125.
- (9) Steensma, M.; Westerterp, K. R. Thermally Safe Operation of a Semibatch Reactor for Liquid-Liquid Reactions. Slow Reactions. *Ind. Eng. Chem. Res.* **1990**, *29*, 1259.
- (10) Steensma, M.; Westerterp, K. R. Thermally Safe Operation of a Semibatch Reactor for Liquid-Liquid Reactions. Fast Reactions. *Chem. Eng. Technol.* **1991**, *14*, 367.
- (11) Maestri, F.; Rota, R. Thermally Safe Operation of Liquid-Liquid Semibatch Reactors. Part I: Single Kinetically Controlled Reactions with Arbitrary Reaction Order. *Chem. Eng. Sci.* **2005**, *60*, 3309.
- (12) Maestri, F.; Rota, R. Thermally Safe Operation of Liquid-Liquid Semibatch Reactors. Part II: Single Diffusion Controlled Reactions with Arbitrary Reaction Order. *Chem. Eng. Sci.* **2005**,

- 1  
2  
3 60, 5590.  
4  
5  
6 (13) Westerterp, K. R.; Molga, E. J. No More Runaways in Fine Chemical Reactors. *Ind. Eng.*  
7  
8 *Chem. Res.* **2004**, *43*, 4585.  
9  
10 (14) Westerterp, K. R.; Molga, E. J. Runaway Prevention in Liquid-Liquid Semibatch Reactors.  
11  
12 *Inzynieria Chemiczna i Procesowa* **2004**, *25*, 2041.  
13  
14  
15 (15) Westerterp, K. R.; Molga, E. J. Safety and Runaway Prevention in Batch and Semibatch  
16  
17 Reactors – A Review. *Chem. Eng. Res. Des.* **2006**, *84*, 543.  
18  
19  
20 (16) van Woezik, B. A. A.; Westerterp, K. R. The Nitric Acid Oxidation of 2-Octanol. A Model  
21  
22 Reaction for Multiple Heterogeneous Liquid-Liquid Reactions. *Chem. Eng. Process.* **2000**,  
23  
24 *39*, 521.  
25  
26  
27 (17) van Woezik, B. A. A.; Westerterp, K. R. Runaway Behavior and Thermally Safe Operation of  
28  
29 Multiple Liquid-Liquid Reactions in the Semibatch Reactor. The Nitric Acid Oxidation of 2-  
30  
31 Octanol. *Chem. Eng. Process.* **2001**, *41*, 59.  
32  
33  
34 (18) Maestri, F.; Re Dionigi, L.; Rota, R.; Lunghi, A.; Gigante, L.; Cardillo, P. Safe and Productive  
35  
36 Operation of Homogeneous Semibatch Reactors. II: the Nitration of N-(2-Phenoxyphenyl)  
37  
38 Methane Sulphonamide. *Ind. Eng. Chem. Res.* **2006**, *45*, 8014.  
39  
40  
41 (19) Maestri, F.; Rota, R. Temperature Diagrams for Preventing Decomposition or Side Reactions  
42  
43 in Liquid-Liquid Semibatch Reactors. *Chem. Eng. Sci.* **2006**, *61*, 3068.  
44  
45  
46 (20) Maestri, F.; Rota, R. Safe and Productive Operation of Homogeneous Semibatch Reactors  
47  
48 Involving Autocatalytic Reactions with Arbitrary Reaction Order. *Ind. Eng. Chem. Res.*  
49  
50 **2007**, *46*, 5333.  
51  
52  
53 (21) Zaldivar, J. M.; Molga, E. J.; Alós, M. A.; Hernández, H.; Westerterp, K. R. Aromatic  
54  
55 Nitrations by Mixed Acids. Slow Liquid-Liquid Reaction Regime. *Chem. Eng. Process.*  
56  
57 **1995**, *34*, 543.  
58  
59  
60 (22) Zaldivar, J. M.; Molga, E. J.; Alós, M. A.; Hernández, H.; Westerterp, K. R. Aromatic  
Nitrations by Mixed Acids. Fast Liquid-Liquid Reaction Regime. *Chem. Eng. Process.*



- 1  
2  
3  
4  
5  
6  
7  
8  
9  
10  
11  
12  
13  
14  
15  
16  
17  
18  
19  
20  
21  
22  
23  
24  
25  
26  
27  
28  
29  
30  
31  
32  
33  
34  
35  
36  
37  
38  
39  
40  
41  
42  
43  
44  
45  
46  
47  
48  
49  
50  
51  
52  
53  
54  
55  
56  
57  
58  
59  
60
- 1996**, 35, 91.
- (23) Zaldivar, J. M.; Barcons, C.; Hernández, H.; Molga, E. J.; Snee, T. J. Modelling and Optimization of Semibatch Toluene Mononitration with Mixed Acid from Performance and Safety Viewpoints. *Chem. Eng. Sci.* **1992**, 47, 2517.
- (24) Marziano, N. C.; Tomasin, A.; Tortato, C.; Zaldivar, J. M. Thermodynamic Nitration Rates of Aromatic Compounds. Part 4. Temperature Dependence in Sulphuric Acid of  $\text{HNO}_3 \rightarrow \text{NO}_2^+$  Equilibrium, Nitration Rates and Acidic Properties of the Solvent. *J. Chem. Soc. Perkin Trans.* **1998**, 2, 1973.
- (25) Zaldivar, J. M.; Alòs, M. A.; Molga, E. J.; Hernandez, H.; Westerterp, K. R. The Effect of Phase Inversion During Semibatch Aromatic Nitrations. *Chem. Eng. Process.* **1995**, 34, 529.
- (26) Zaldivar, J. M.; Hernandez, H.; Nieman, H.; Molga, E. J.; Bassani, C. The FIRES Project: Experimental Study of Thermal Runaway Due to Agitation Problems During Toluene Nitration. *J. Loss Prev.* **1993**, 6, 319.
- (27) Benuzzi, A.; Zaldivar, J. M. *Safety of Chemical Batch Reactors and Storage Tanks*; Kluwer Academic Publishers: Dordrecht, 1991.
- (28) Westerterp, K. R.; van Swaaij, W. P. M.; Beenackers, A. A. C. M. *Chemical reactor design and operation*; John Wiley & Sons: Chichester, 1984.
- (29) Cardillo, P. *Incidenti in Ambiente Chimico. Guida allo studio e alla valutazione delle reazioni fugitive*; Stazione Sperimentale per i Combustibili: San Donato Milanese, 1998.
- (30) Perry, R. H.; Green, D. W. *Perry's Chemical Engineer's Handbook*; Mc Graw-Hill International Editors: New York, 1998.
- (31) Varma, A.; Morbidelli, M.; Wu, H. *Parametric Sensitivity in Chemical Systems*; University Press: Cambridge, 1999.
- (32) Seaton, W. H.; Freedman, E.; Treweek, D. N. CHETAH – The ASTM Chemical Thermodynamics and Energy Release Potential Evaluation Program, ASTM DS51, Philadelphia, PA, 1974.

- 1  
2  
3 (33) Alós, M. A.; Nomen, R.; Sempere, J. M.; Strozzi, F.; Zaldívar, J. M. Generalized Criteria for  
4  
5 Boundary Safe Conditions in Semibatch Processes: Simulated Analysis and Experimental  
6  
7 Results. *Chem. Eng. Process.* **1998**, *37*, 405.  
8  
9  
10 (34) Morbidelli, M.; Varma, A. A Generalized Criterion for Parametric Sensitivity: Application to  
11  
12 Thermal Explosion Theory. *Chem. Eng. Sci.* **1998**, *43*, 91.  
13  
14  
15 35) Strozzi, F.; Zaldívar, J. M.; Kronberg, A. E.; Westerterp, K. R. On-line Runaway Detection in  
16  
17 Batch Reactors Using Chaos Theory Techniques. *AIChE J.* **1999**, *45*, 2429.  
18  
19  
20 (36) Zaldívar, J. M.; Cano, J. Alós, M. A.; Sempere, J. M.; Nomen, R.; Lister, D.; Maschio, G.;  
21  
22 Obertopp, T.; Gilles, E. D.; Bosch, J.; Strozzi, F. A General Criterion to Define Runaway  
23  
24 Limits in Chemical Reactors. *J. Loss. Prev.* **2003**, *16*, 187.  
25  
26  
27 (37) Bosch, J.; Strozzi, F.; Zbilut, J. P.; Zaldívar, J. M. On-line Runaway Detection in Isoperibolic  
28  
29 Batch and Semibatch Reactors Using the Divergence Criterion. *Comput. Chem. Eng.* **2004**,  
30  
31 28, 527.  
32  
33  
34 (38) Zaldívar, J. M.; Bosch, J.; Strozzi, F.; Zbilut, J. P. Early Warning Detection of Runaway  
35  
36 Initiation Using Non-linear Approaches. *Nonlin. Sci. Num. Sim.* **2005**, *10*, 299.  
37  
38  
39  
40  
41  
42  
43  
44  
45  
46  
47  
48  
49  
50  
51  
52  
53  
54  
55  
56  
57  
58  
59  
60

Starting temperature:	141 °C
Starting pressure:	1.64 bar a
Starting self heating rate:	0.384 °C/min
Final instrumental temperature:	255 °C
Final instrumental pressure:	46.87 bar a
Instrumental adiabatic temperature rise:	114 °C
Calorimeter thermal inertia factor:	2.846
Adiabatic temperature rise:	325 °C
Final reaction temperature:	466 °C
Decomposition enthalpy:	-438 kJ/kg
Time to Maximum Rate (TMR):	5 h 45 min

Table 1. ARC test on final reacting mixture: thermodynamic properties of reaction mass decomposition.

<i>Dimensional parameters</i>	<i>Dimensionless parameters</i>
$(UA)_0 = 2.487 \text{ W/K}$	$\Psi_{EMAT} = 1.27$
$\tilde{\rho}_c = 1787 \text{ kg/m}^3$	$E_{x,EMAX} = 8.20$
$\tilde{\rho}_d = 1353 \text{ kg/m}^3$	$Co_{MIN} = 4.50$
$\tilde{C}_{P,c} = 1.477 \text{ kJ/(kg K)}$	$\gamma = 35$
$\tilde{C}_{P,d} = 0.8690 \text{ kJ/(kg K)}$	$\Delta\tau_{ad,0} = 0.430$
$V_c = 382.9 \text{ cm}^3$	$\varepsilon = 0.348$
$V_D = 143.4 \text{ cm}^3$	
$T_0 = 37^\circ\text{C}$	
$\Delta T_{ad,0} = 129^\circ\text{C}$	$R_y = 0.0623$
$t_D = 636 \text{ s}$	$R_{y,QFS} = 0.0550$
$C_{HNO_3,0} = 2.764 \text{ kmol/m}^3$	
$m_{4-chloro BTf} = 0.01$	

Table 2 Operating parameters for isoperibolic RC1 experiment.

<i>Dimensional parameters</i>	<i>Dimensionless parameters</i>
$(UA)_0 = 4910 \text{ W/K}$	$\Psi_{EMAT} = 1.27$
$\tilde{\rho}_c = 1787 \text{ kg/m}^3$	$E_{x,EMAX} = 8.20$
$\tilde{\rho}_d = 1353 \text{ kg/m}^3$	$Co_{MIN} = 4.50$
$\tilde{C}_{P,c} = 1.477 \text{ kJ/(kg K)}$	$\gamma = 35$
$\tilde{C}_{P,d} = 0.869 \text{ kJ/(kg K)}$	$\Delta\tau_{ad,0} = 0.430$
$V_c = 4.688 \text{ m}^3$	$\varepsilon = 0.348$
$V_D = 1.633 \text{ m}^3$	
$T_0 = 37^\circ\text{C}$	
$\Delta T_{ad,0} = 129^\circ\text{C}$	$R_y = 0.387$
$t_D = 3946 \text{ s}$	$R_{y,QFS} = 0.0550$
$C_{HNO_3,0} = 2.764 \text{ kmol/m}^3$	
$m_{4-chloro BTf} = 0.01$	

Table 3. Operating parameters for industrial reactor.

Parameters	Checks
relative uncertainty	
(UA) <sub>0</sub>	$R_{y,calc}(t_{D,MIN,calc}) > \frac{(1 - \varepsilon \cdot S_{R_y,QFS/Co}) \cdot [(1 - \varepsilon) \cdot Co_{MIN,calc} + R_H]}{Co_{MIN,calc} + R_H} \cdot R_{y,QFS}(Co_{MIN,calc})$
ε= 0.05	0.387 > 0.0549
ε= 0.1	0.387 > 0.0547
Δτ <sub>ad,0</sub>	$R_{y,calc}(t_{D,MIN,calc}) > R_{y,QFS}(Co_{MIN,calc})$
	$\varepsilon < \frac{toll}{1 - toll} \cdot \frac{1}{S_{\psi/Ex}}$
ε= 0.05	0.387 > 0.0550      0.05 < 0.371
ε= 0.1	0.387 > 0.0550      0.1 < 0.371
γ	$R_{y,calc}(t_{D,MIN,calc}) > \exp\left(\varepsilon \cdot \frac{\gamma_{calc}}{\tau_{cool}}\right) \cdot R_{y,QFS}(Co_{MIN,calc})$
	$\varepsilon < \frac{toll}{1 - toll} \cdot \frac{1}{S_{\psi/Ex}}$
ε= 0.05	0.387 > 0.299
ε= 0.1	0.387 < 1.63
A	$R_{y,calc}(t_{D,MIN,calc}) > \frac{1}{1 - \varepsilon} \cdot R_{y,QFS}(Co_{MIN,calc})$
ε= 0.05	0.387 > 0.0579
ε= 0.1	0.387 > 0.0611
n	$R_{y,calc}(t_{D,MIN,calc}) > (C_{HNO_3,0} \cdot m_{4-Cl-BTF})^{\varepsilon \cdot n_{calc}} \cdot (1 - \varepsilon \cdot S_{R_y,QFS/n}) R_{y,QFS}(Co_{MIN,calc})$
	0.387 > 0.0471
ε= 0.05	0.387 > 0.0403
ε= 0.1	

Table 4. Checks, for heterogeneous L-L kinetically controlled SB systems, on experimental parameters subjected to a degree of uncertainty ε. In order to consider safe operating conditions selected using TRC and ISC optimization – scale-up procedure all checks must be positive.

<i>Sensitivity Index</i>	$Co < 5$	$Co > 5$
$S_{R_{y,QFS} / Co}$ S ( $Co_{MIN}=4.5$ )=	$0.0007 \cdot \frac{Co}{0.0007 \cdot Co + 0.0519}$ 0.0571	$\frac{-0.0241}{-0.0241 \cdot \ln(Co) + 0.094187}$
$S_{R_{y,QFS} / n}$	-0.469	-0.469
	$0 < E_X < 2$	$2 < E_X < 30$
$S_{\Psi / E_X}$ S ( $E_{X,EMAX}=8.2$ )=	$\frac{-1 \cdot 10^{-2} \cdot E_X^2 + 8.91 \cdot 10^{-2} \cdot E_X}{-1 \cdot 10^{-2} \cdot E_X^2 + 8.91 \cdot 10^{-2} \cdot E_X + 1}$	$\frac{-3.72 \cdot 10^{-4} \cdot E_X^2 + 2.50 \cdot 10^{-2} \cdot E_X}{-3.72 \cdot 10^{-4} \cdot E_X^2 + 2.50 \cdot 10^{-2} \cdot E_X + 1.09}$ 0.142

Table 5. Sensitivity coefficients of  $R_{y,QFS}$  with respect to different dimensionless parameters ( $Co$ ,  $n$  and  $E_X$ ) for heterogeneous L-L kinetically controlled SB systems derived from analytical interpolation of the curves in Figures 1 and 2.

1  
2  
3  
4  
5  
6  
7  
8  
9  
10  
11  
12  
13  
14  
15  
16  
17  
18  
19  
20  
21  
22  
23  
24  
25  
26  
27  
28  
29  
30  
31  
32  
33  
34  
35  
36  
37  
38  
39  
40  
41  
42  
43  
44  
45  
46  
47  
48  
49  
50  
51  
52  
53  
54  
55  
56  
57  
58  
59  
60

### Captions to the figures.

Figure 1. Inherently safe conditions of heterogeneous (liquid-liquid) SBRs in which a single non-autocatalytic slow reaction in the continuous phase occurs. Influence of the cooling number,  $Co$ , on the  $R_{y,QFS}$  parameter.  $R_H=1$ .  $0.02 < Da < 20$ ,  $0.05 < \varepsilon < 0.6$ ,  $30 < \gamma < 45$ ,  $0.1 < \Delta\tau_{ad,0} < 0.7$ . Representation of the laboratory and scaled-up operating conditions.

Figure 2. Inherently safe conditions of SBRs in which a single exothermic reaction is carried out. Influence of the exothermicity number,  $E_x$ , on the maximum temperature rise  $\psi = (T_{max}/T_0)_{max}$ .  $R_H=1$ .  $2 < Co < 80$ ,  $0.75 < n < 2$ ,  $0.02 < Da < 20$ ,  $0.05 < \varepsilon < 0.6$ ,  $30 < \gamma < 45$ ,  $0.1 < \Delta\tau_{ad,0} < 0.7$ . Representation of the laboratory operating conditions and identification of the maximum exothermicity number,  $E_{x,MAX}$ , during the scale-up process. Straight line represents the dimensionless initial target temperature equations  $\frac{\tau_{ta,0}}{\tau_0} = 1 + 1.05 \frac{\tau_0}{\gamma} E_x$  with  $\tau_0$  and  $\gamma$  in usual industrial ranges.

Figure 3. (A) DSC thermal characterization of 4-chloro BTF in nitrogen. Sample amount: 3.57mg; heating rate: 10°C/min; temperature range: 30-280°C.

(B) DSC thermal characterization of 4-chloro BTF in static air. Sample amount: 3.81mg; heating rate: 10°C/min; temperature range: 30-280°C.

(C) DSC thermal characterization of 4-chloro, 3-nitro BTF in nitrogen. Sample amount: 3.92mg; heating rate: 10°C/min; temperature range: 30-280°C.

(D) DSC thermal characterization of 4-chloro, 3-nitro BTF in static air. Sample amount: 3mg; heating rate: 10°C/min; temperature range: 30-280°C.

Figure 4. ARC thermal characterization of final reaction mixture. Sample amount: 2.55g. Initial temperature: 30°C.

Figure 5. Adiabatic (ARC) experiments at different stirring rate for the determination of the reaction microkinetics.

Figure 6. Adiabatic (RC1) experiment for the determination of the reaction microkinetics. Stirring speed: 500rpm. Experimental and best fit temperature-time profiles.

Figure 7. Experimental and simulated temperature-time profiles for operating conditions individuated from optimization procedure at the RC1 scale.



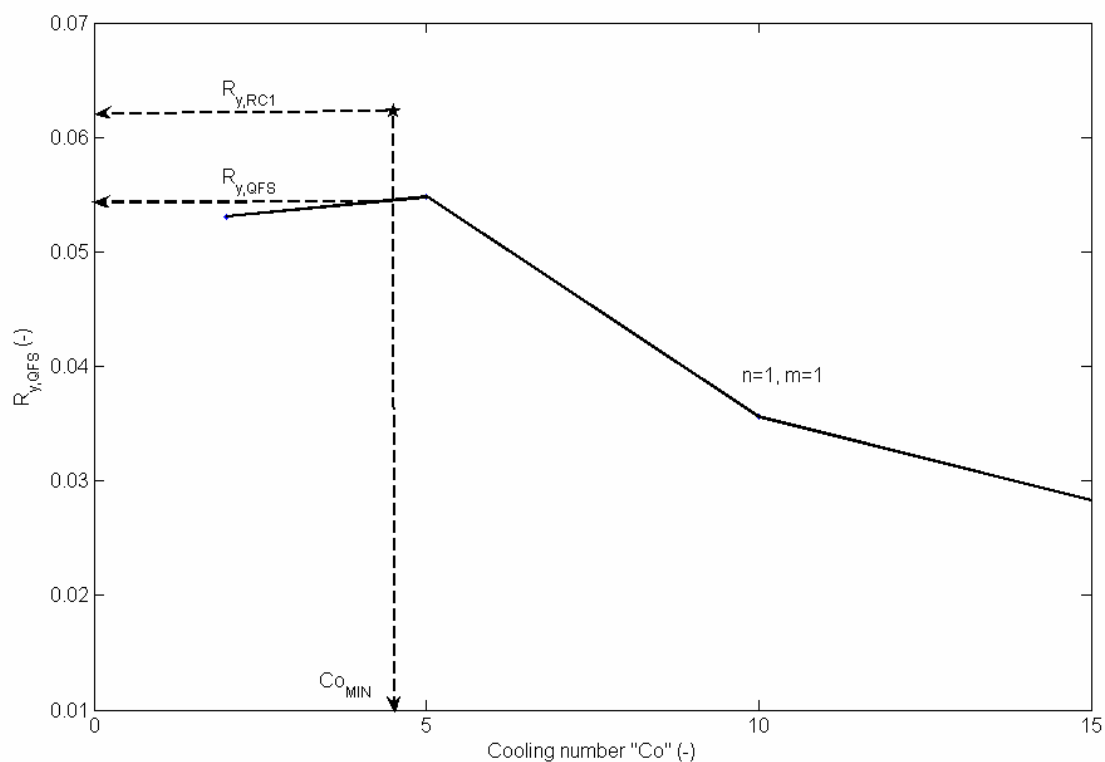


Figure 1. Inherently safe conditions of heterogeneous (liquid-liquid) SBRs in which a single non-autocatalytic slow reaction in the continuous phase occurs. Influence of the cooling number,  $Co$ , on the  $R_{y,QFS}$  parameter.  $R_H=1$ .  $0.02 < Da < 20$ ,  $0.05 < \varepsilon < 0.6$ ,  $30 < \gamma < 45$ ,  $0.1 < \Delta\tau_{ad,0} < 0.7$ . Representation of the laboratory and scaled-up operating conditions.

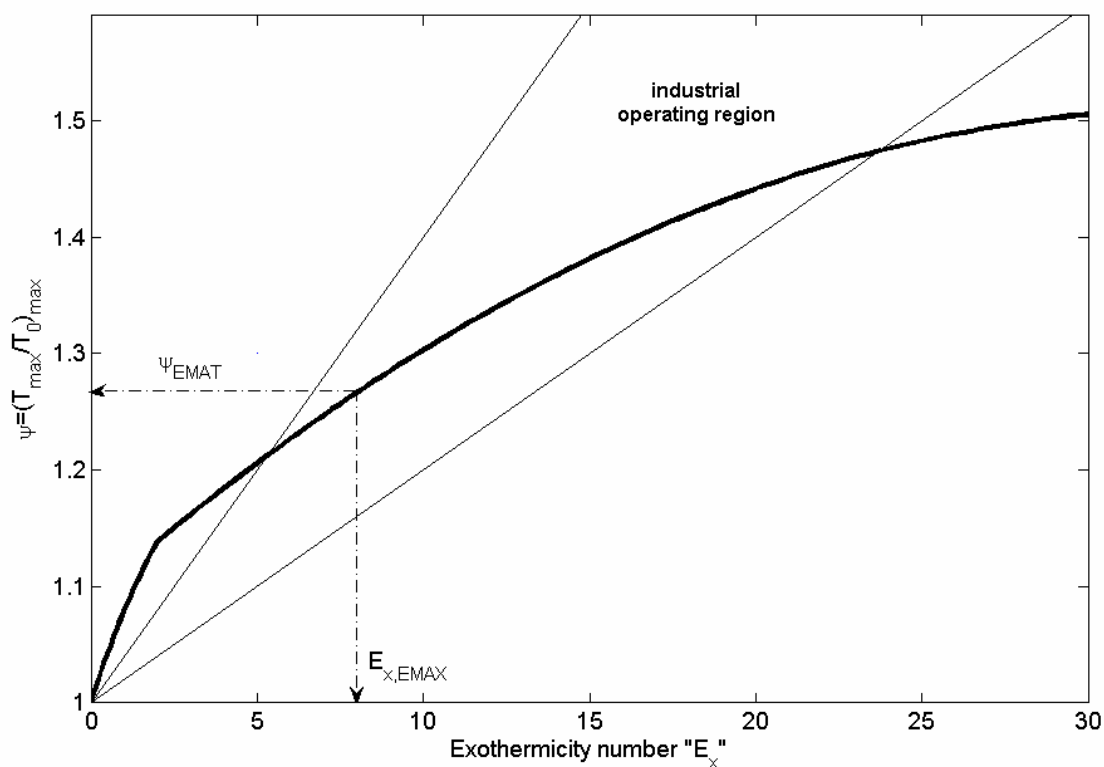


Figure 2. Inherently safe conditions of SBRs in which a single exothermic reaction is carried out. Influence of the exothermicity number,  $E_x$ , on the maximum temperature rise  $\psi = (T_{\max}/T_0)_{\max}$ .  $R_H=1$ .  $2 < Co < 80$ ,  $0.75 < n < 2$ ,  $0.02 < Da < 20$ ,  $0.05 < \varepsilon < 0.6$ ,  $30 < \gamma < 45$ ,  $0.1 < \Delta\tau_{ad,0} < 0.7$ . Representation of the laboratory operating conditions and identification of the maximum exothermicity number,  $E_{x,MAX}$ , during the scale-up process. Straight lines represent minimum and maximum dimensionless initial target temperature equations  $\frac{\tau_{ta,0}}{\tau_0} = 1 + 1.05 \frac{\tau_0}{\gamma} E_x$  with  $\tau_0$  and  $\gamma$  in usual industrial ranges.

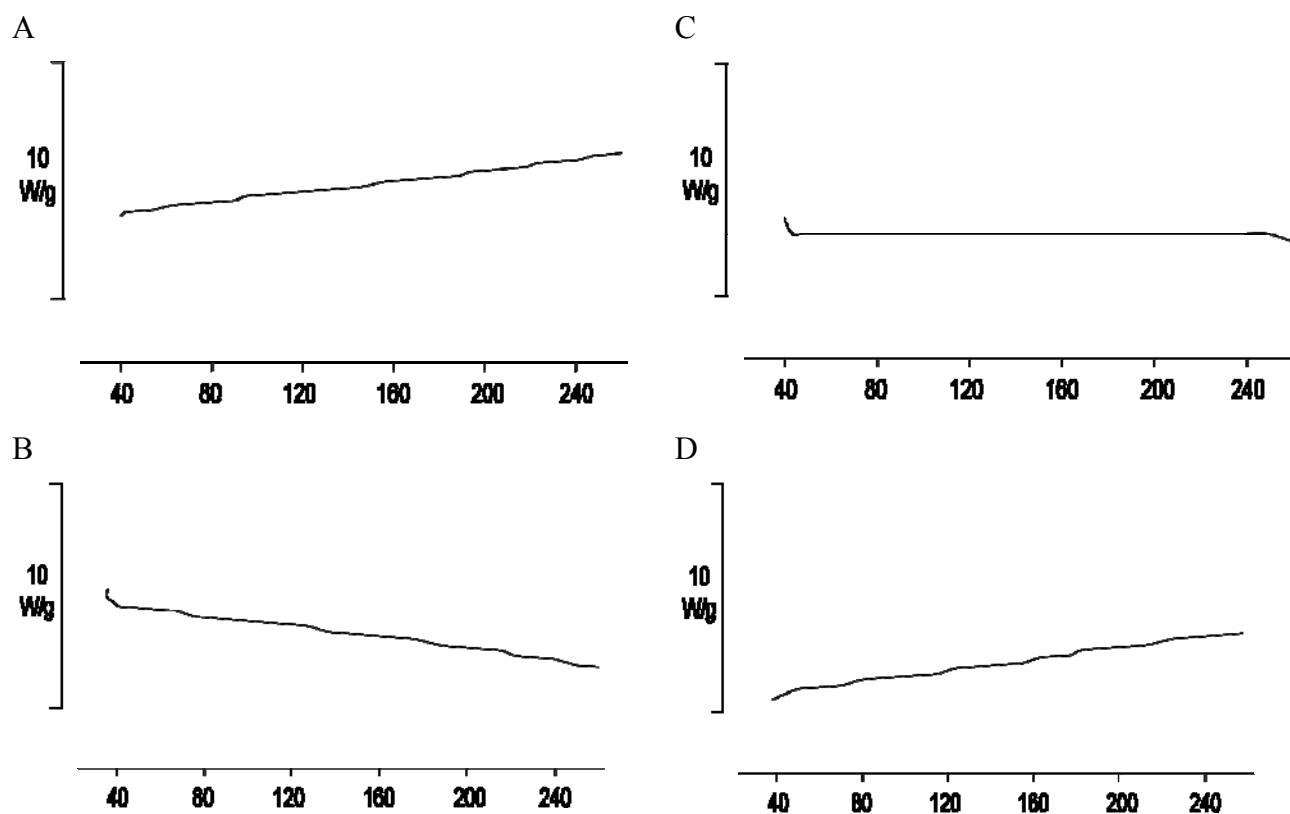


Figure 3. (A) DSC thermal characterization of 4-chloro BTF in nitrogen. Sample amount: 3.57mg; heating rate: 10°C/min; temperature range: 30-280°C.

(B) DSC thermal characterization of 4-chloro BTF in static air. Sample amount: 3.81mg; heating rate: 10°C/min; temperature range: 30-280°C.

(C) DSC thermal characterization of 4-chloro, 3-nitro BTF in nitrogen. Sample amount: 3.92mg; heating rate: 10°C/min; temperature range: 30-280°C.

(D) DSC thermal characterization of 4-chloro, 3-nitro BTF in static air. Sample amount: 3mg; heating rate: 10°C/min; temperature range: 30-280°C.

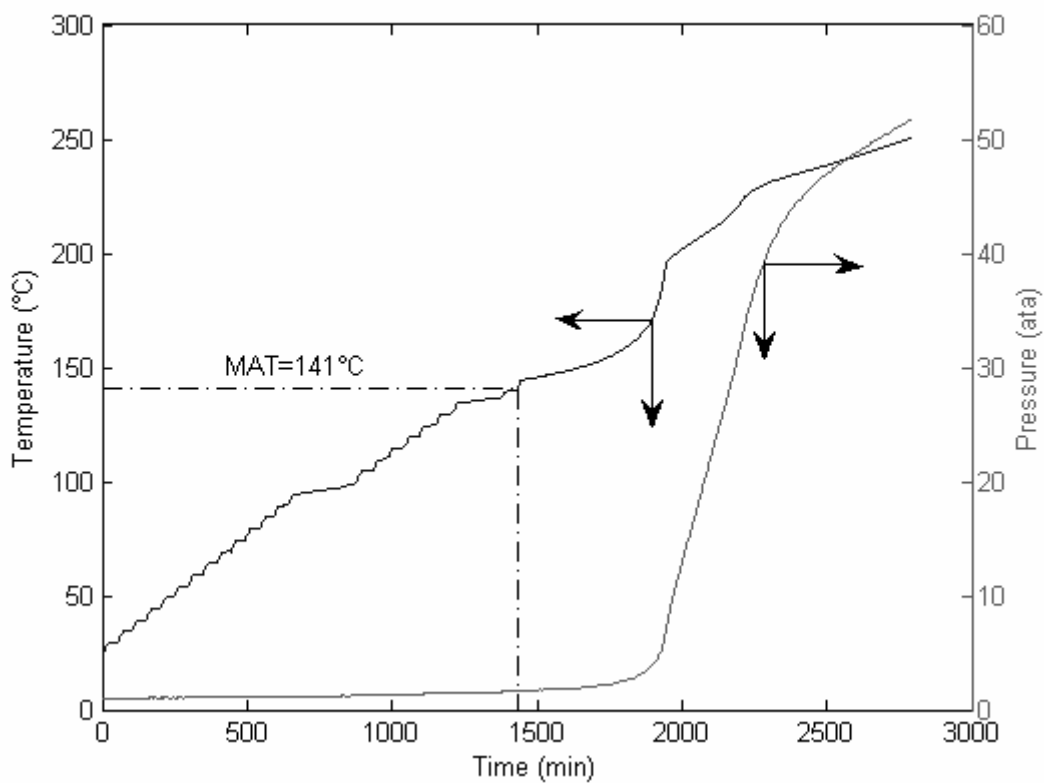


Figure 4. ARC thermal characterization of the final reaction mixture. Sample amount: 2.55g. Initial temperature: 30°C.

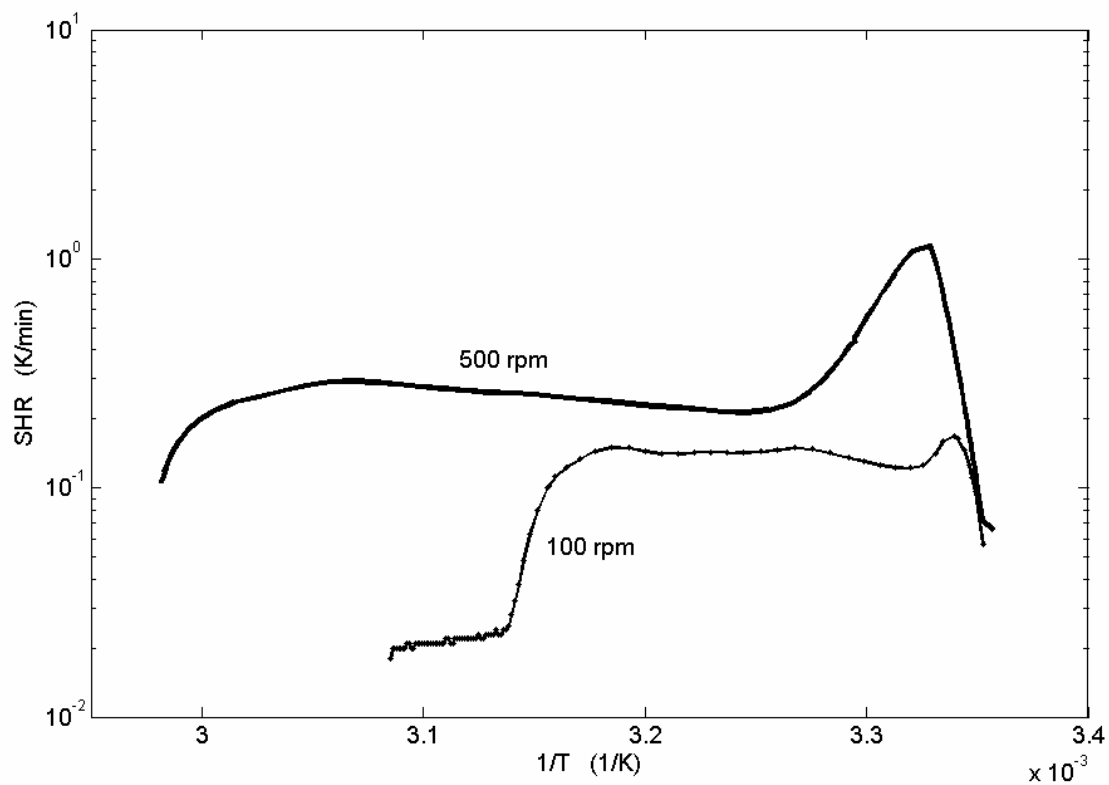


Figure 5. Adiabatic (ARC) experiments at different stirring rate for the determination of the reaction microkinetics.

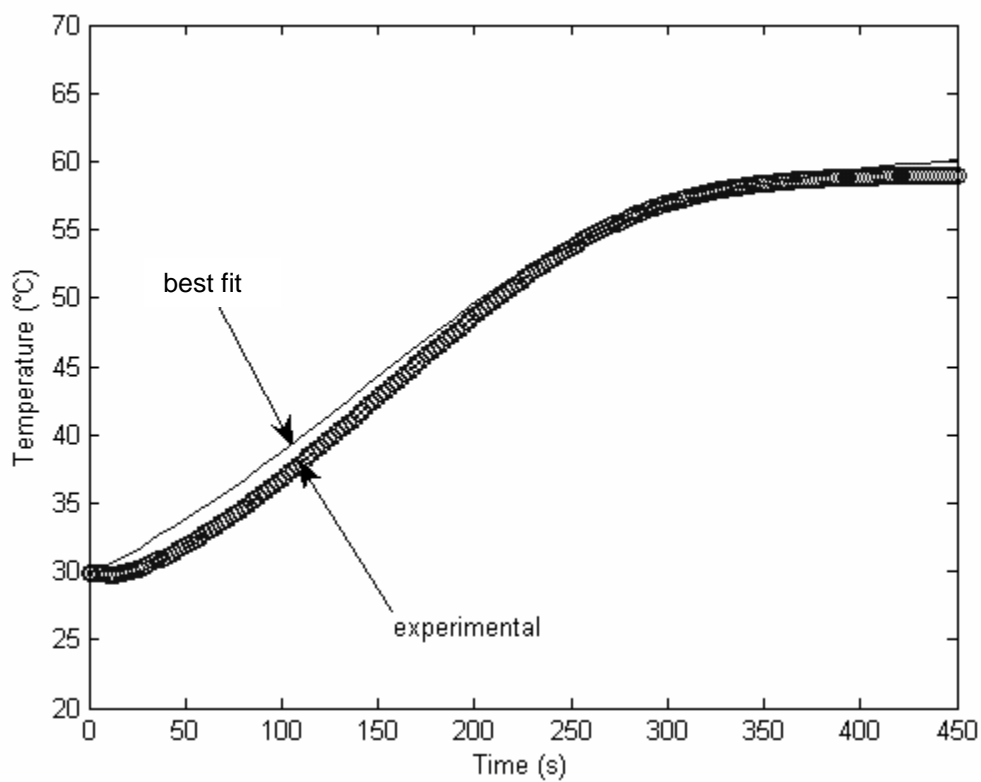


Figure 6. Adiabatic (RC1) experiment for the determination of the reaction microkinetics. Stirring speed: 500rpm. Experimental and best fit temperature-time profiles.

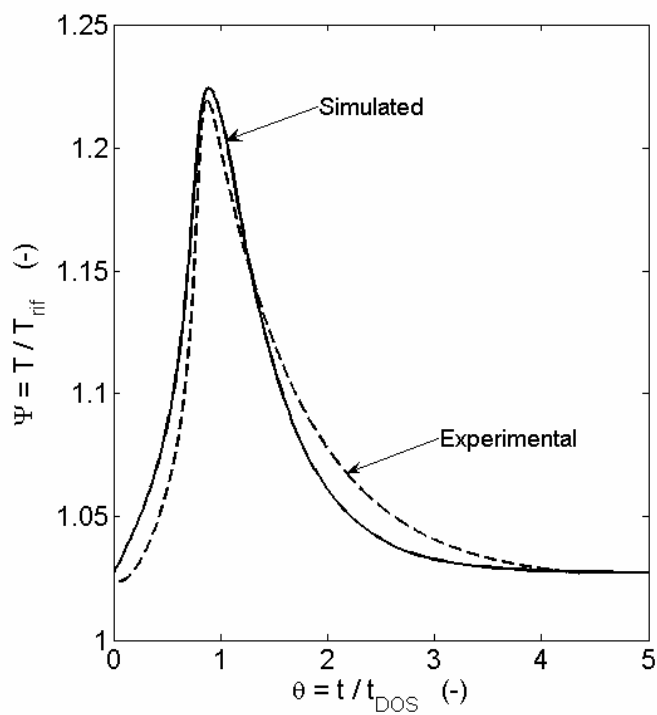


Figure 7. Experimental and simulated temperature-time profiles for operating conditions individuated from optimization procedure at the RC1 scale.